Supplementary material

Table S1. List of ion masses and molecular formulae measured with the PTR-TOF-MS. The fragmentation rates of each molecule at a given field density ratio (E/N) were used to calculate the reaction rates of the parent ions. The most probable molecule structure, thus compound name, in the first column was retrieved from the direct calibration, from GC-MS analyses conducted at the study site in 2012 or from the literature on poplar leaf emissions and similar eddy covariance studies. The natural abundance (%) of each protonated molecule containing ^{1}H, ^{12}C, ^{14}N, and ^{16}O can be used to correct the BVOC fluxes and take into account the amounts of molecules containing isotopes ^{2}H, ^{13}C, ^{15}N, ^{17}O, and ^{18}O.

| Most probable compound structure	Molecular formula of the protonated compound	Peak centre (protonated molecular mass)	Abundance ratio (%)
Formaldehyde	$(CH_2O)H^+$	31.0178	98.6639
Methanol	$(CH_4O)H^+$	33.0335	98.6414
Acetonitrile	$(C_2H_3N)H^+$	42.0338	97.4866
Propene	$(C_3H_6)H^+$	43.0542	96.7703
Acetaldehyde	$(C_2H_4O)H^+$	45.0335	97.5938
Formic acid	$(CH_2O_2)H^+$	47.0128	98.4243
Ethanol	$(C_2H_6O)H^+$	47.0491	97.5715
Acetone	$(C_3H_6O)H^+$	59.0491	96.5353
Acetic acid (+ fragment)	$(C_2H_4O_2)H^+$	61.0284	97.3568
	$(C_2H_2O)H^+$	43.0178	97.6161
Isoprene (+ fragment)	$(C_5H_8)H^+$	69.0699	94.7041
	$(C_3H_4)H^+$	41.0386	96.7924
Methyl vinyl ketone + methacrolein	$(C_4H_6O)H^+$	71.0491	95.5101
Methyl ethyl ketone	$(C_4H_8O)H^+$	73.0648	95.4882
Benzene	$(C_6H_6)H^+$	79.0542	93.7198
Pentenone	$(C_5H_8O)H^+$	85.0648	94.4741
Pentenol	$(C_5H_{10}O)H^+$	87.0804	94.4525
Pentanol (+ fragment)	$(C_5H_{12}O)H^+$	89.0961	94.4310
	$(C_5H_{10})H^+$	71.0855	94.6825
Toluene + cymene	$(C_7H_8)H^+$	93.0699	92.7033
Furfural	$(C_5H_4O_2)H^+$	97.0290	94.2878
Hexenal (+ fragments)	$(C_6H_{10}O)H^+$	99.0804	93.4495
	$(C_6H_8)H^+$	81.0699	93.6984
	$(C_3H_4O)H^+$	57.0335	96.5573
Hexenol + hexanal (+ fragment)	$(C_6H_{12}O)H^+$	101.0961	93.4281
	$(C_6H_{10})H^+$	83.0855	93.6769
Hexanol (+ fragment)	$(C_6H_{14}O)H^+$	103.1117	93.4067
	$(C_6H_{12})H^+$	85.1012	93.6555
Styrene	$(C_8H_8)H^+$	105.0699	91.7188
Benzaldehyde	$(C_7H_6O)H^+$	107.0491	92.4993
Xylene	$(C_8H_{10})H^+$	107.0855	91.6978
Benzoic acid	$(C_7H_6O_2)H^+$	123.0441	92.2747
Octenal	$(C_8H_{14}O)H^+$	127.1117	91.4333
Monoterpenes (+ fragments)	$(C_{10}H_{16})H^+$	137.1325	89.6990
	$(C_7H_{10})H^+$	95.0855	92.6821
	$(C_6H_8)H^+$	81.0699	93.6984
Hexyl acetate	$(C_8H_{16}O_2)H^+$	145.1223	91.1904
Dimethyl nonatriene (DMNT)	$(C_{11}H_{18})H^+$	151.1481	88.7261
Methyl salicylate	$(C_8H_8O_3)H^+$	153.0546	91.0522
Monoterpene alcohol	$(C_{10}H_{18}O)H^+$	155.1430	89.4607
Ethyl salicylate	$(C_9H_{10}O_3)H^+$	167.0703	90.0646
Sesquiterpenes (+ fragment)	$(C_{15}H_{24})H^+$	205.1951	84.9583
	$(C_8H_{14})H^+$	111.1168	91.6559
Jasmonic acid	$(C_{12}H_{18}O_3)H^+$	211.1329	87.1458
Ionol	$(C_{15}H_{24}O)H^+$	221.1900	84.7520
Methyl jasmonate	$(C_{13}H_{20}O_3)H^+$	225.1485	86.2006
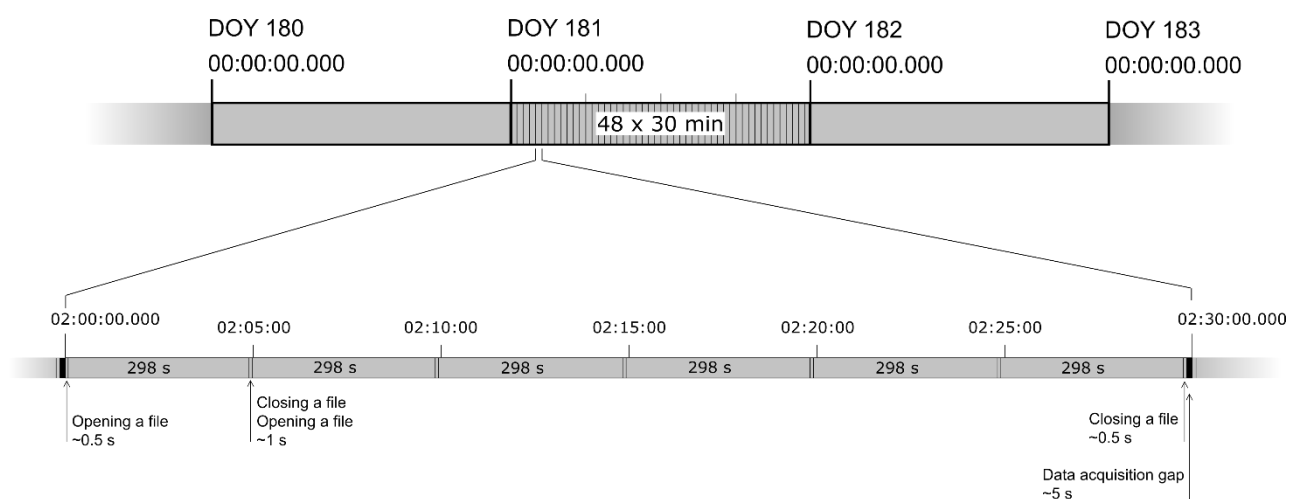
Figure S1. Scheme of volatile organic compound data acquisition with the PTR-TOF-MS. Detailed timing during a 30-min step of recording files, data loss during closing and opening files, and the data acquisition gap added at the end of the 30 min to match the data acquisition of the following 30 min step to the computer clock. The data were recorded in six subsequent 298 s files each half hour. Due to the large size of the data files (50-60 Mb), closing and starting a new data file generated a data gap of ~1 s. At the end of each half hour, a recording gap of ~5 s was allowed to adjust for these delays, so the next file corresponding to the following half hour would start matching the clock at HH:00 or HH:30, as set up in the automated recording algorithm.
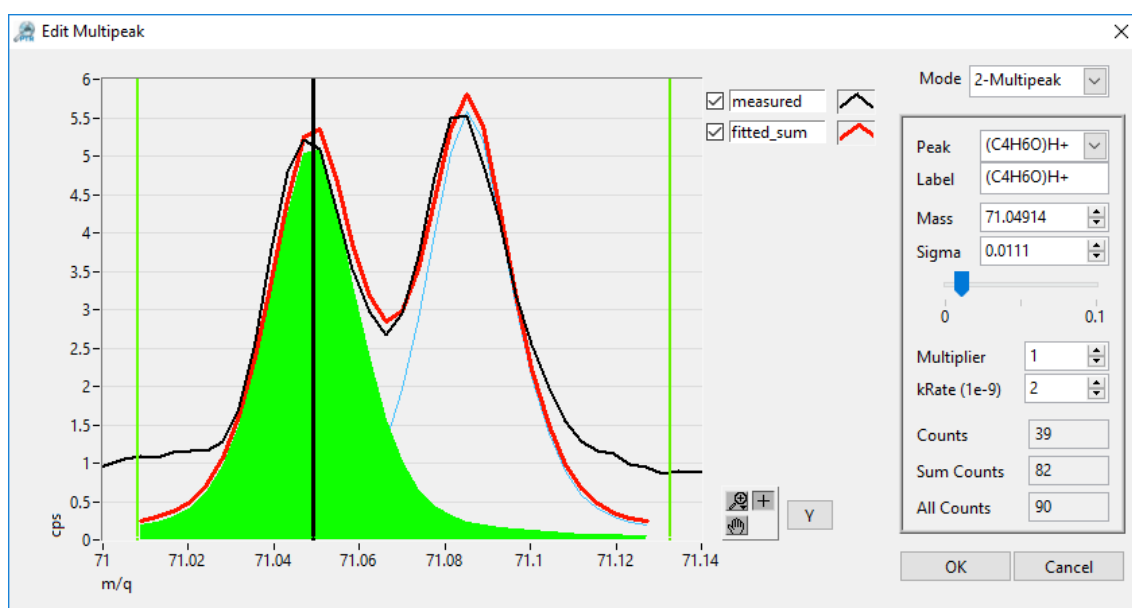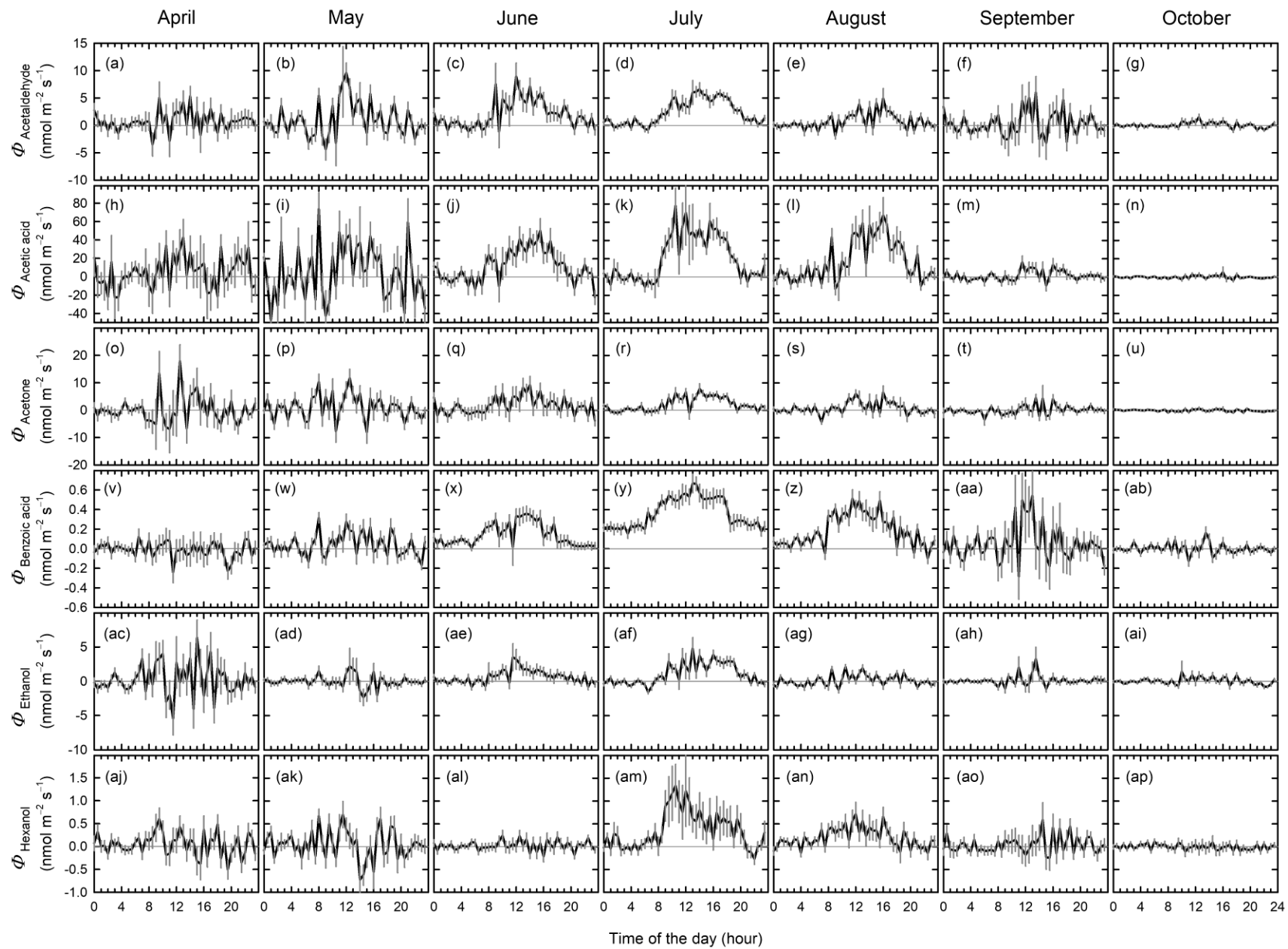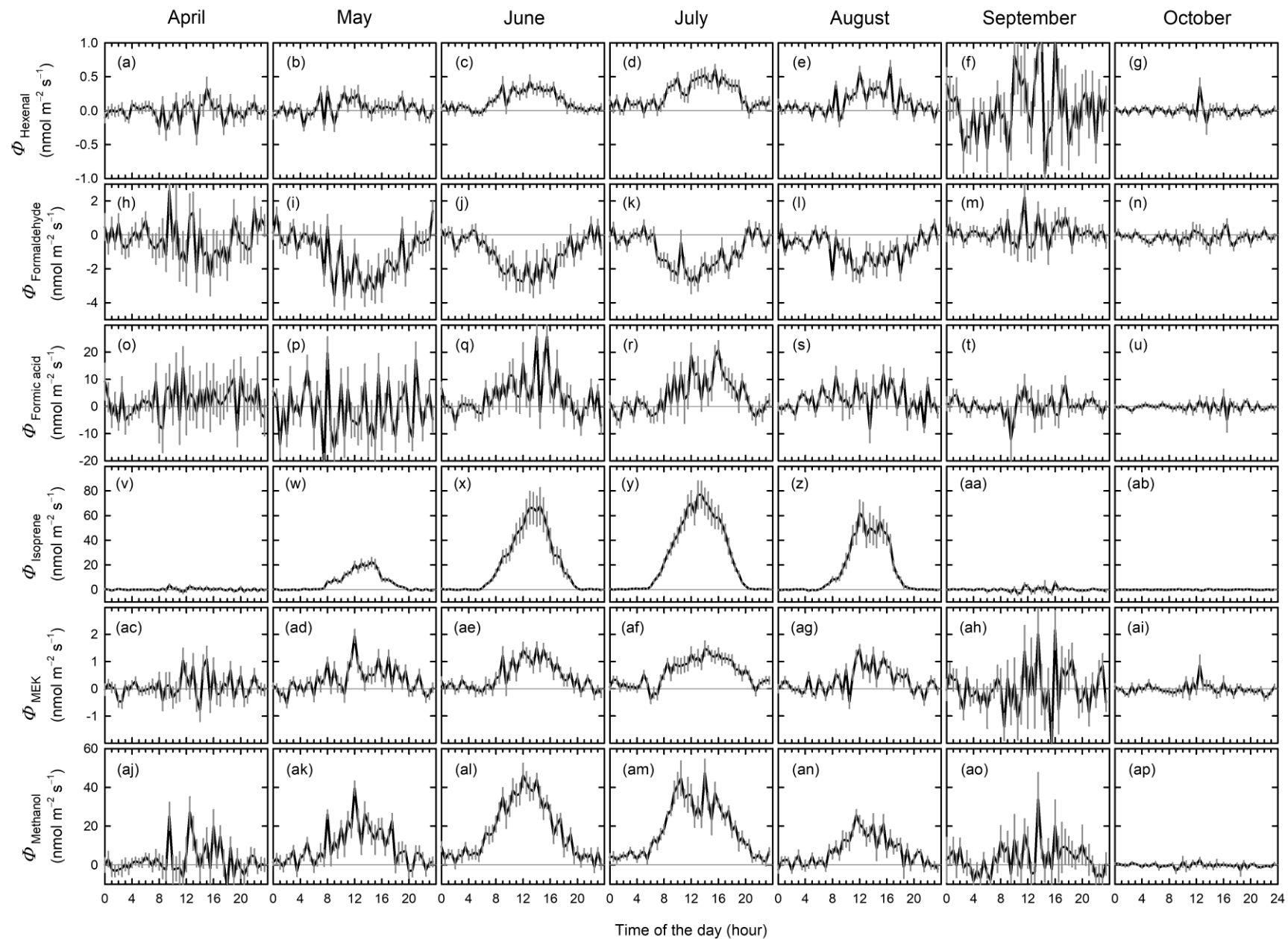
Figure S2. Example of analysis of a multipeak with the "Multipeak" built-in tool in the software PTR-MS Viewer v3.2 (Ionicon, Innsbruck, Austria). In this example, ions $(C_4H_6O)H^+$ and $(C_5H_{10})H^+$ with adjacent peak centres at *m/z* 71.0491 and 71.0855, have overlapping peak tails. The tool allows to match the signal of both ions (in green and blue) to the measured signal (in counts per second) in an average spectrum (black line). The sigma of the Gaussian curve is tuned to match the sum of the signals of both ions (in red) to the measured data. These fitting parameters are used afterwards to calculate the concentrations of both ions independently.
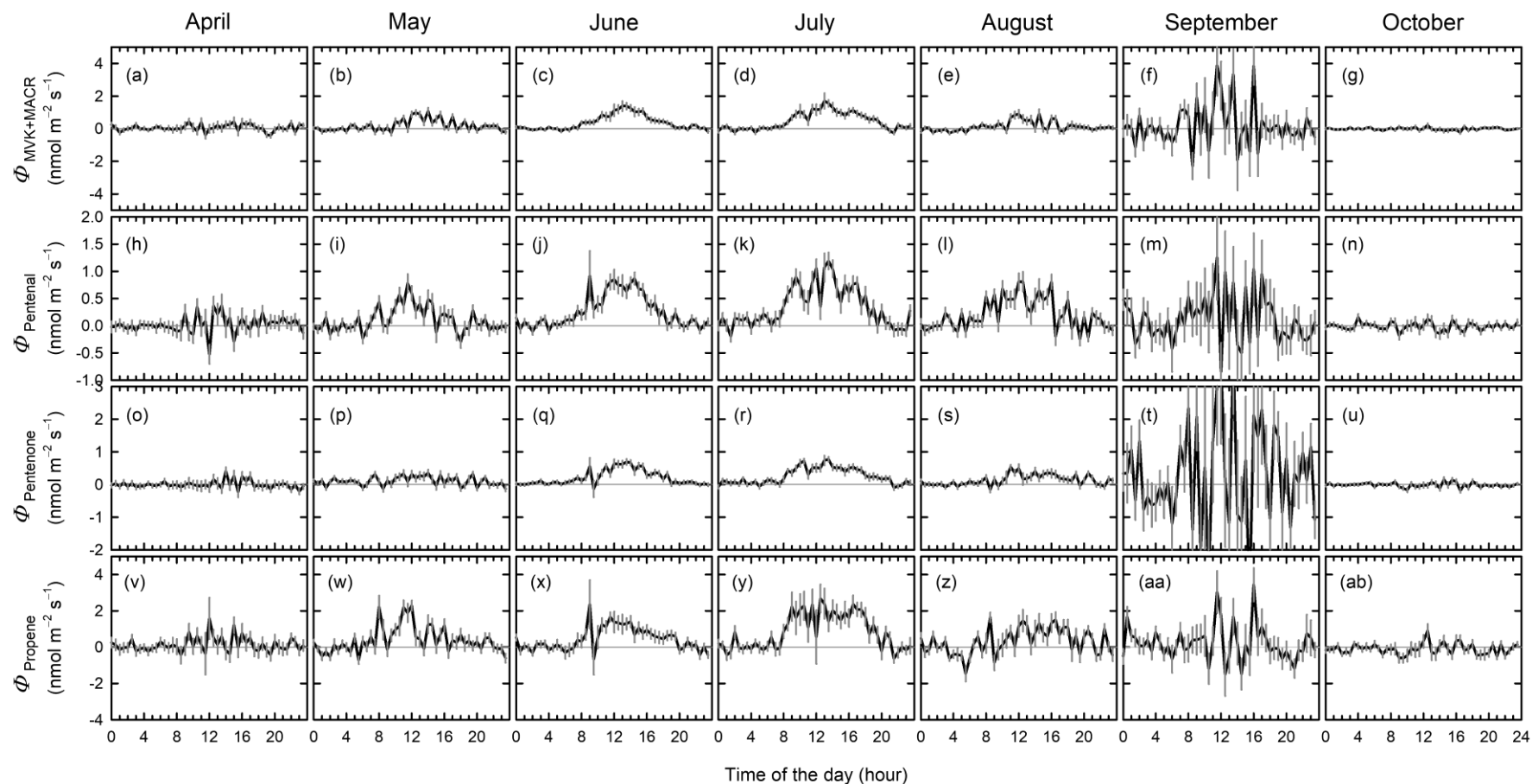
April May June July August September October

Rows (top to bottom):
- $\Phi_{Acetaldehyde}$ (nmol m^{-2} s^{-1}): (a) (b) (c) (d) (e) (f) (g)
- $\Phi_{Acetic\ acid}$ (nmol m^{-2} s^{-1}): (h) (i) (j) (k) (l) (m) (n)
- $\Phi_{Acetone}$ (nmol m^{-2} s^{-1}): (o) (p) (q) (r) (s) (t) (u)
- $\Phi_{Benzoic\ acid}$ (nmol m^{-2} s^{-1}): (v) (w) (x) (y) (z) (aa) (ab)
- $\Phi_{Ethanol}$ (nmol m^{-2} s^{-1}): (ac) (ad) (ae) (af) (ag) (ah) (ai)
- $\Phi_{Hexanol}$ (nmol m^{-2} s^{-1}): (aj) (ak) (al) (am) (an) (ao) (ap)

Time of the day (hour)

4

Figure S3. Diurnal trends per month of BVOC emissions at the poplar short-rotation plantation in year 2015. Average ± SE (n = days of month).

Figure S4. Diurnal trends per month of BVOC emissions at the poplar short-rotation plantation in year 2015. Average ± SE (n = days of month).

Figure S5. Diurnal trends per month of BVOC emissions at the poplar short-rotation plantation in year 2015. Average ± SE (n = days of month).
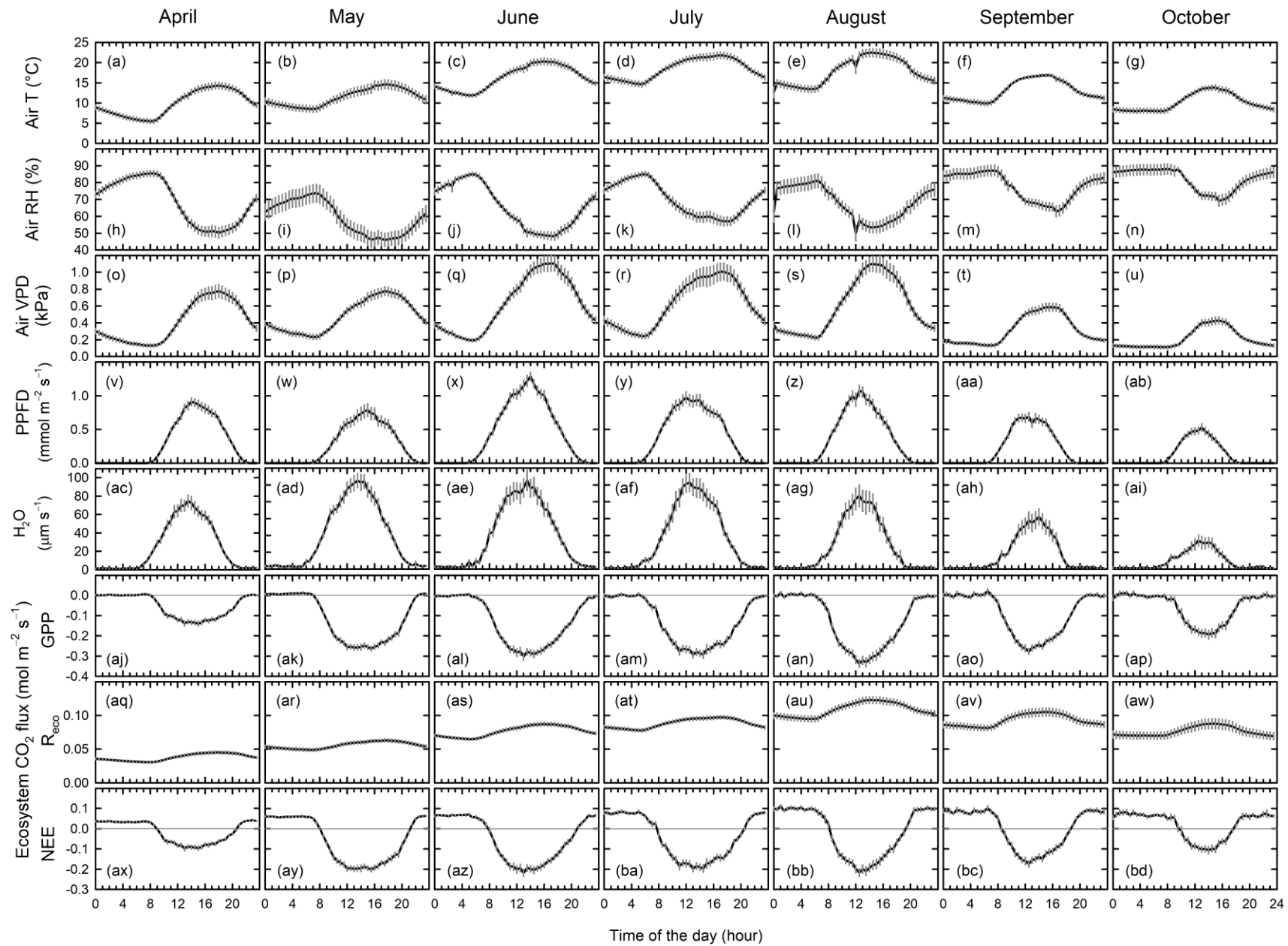
Time of the day (hour)

Figure S6. Diurnal trends per month of environmental parameters, water and CO_2 fluxes as GPP (gross primary production), R_{eco} (ecosystem respiration), and NEE (net ecosystem exchange). Average ± SE (n = days of month).
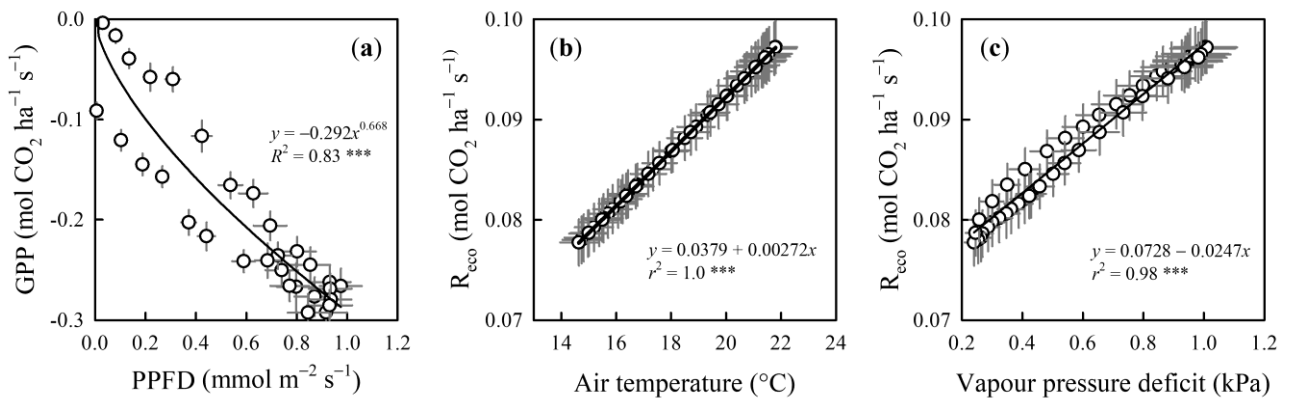

Figure S7. Correlations between CO_2 fluxes and environmental parameters in July 2015. Dots are the monthly-averaged half-hourly values of each day; bars represent the standard error (n = 31 days) of each half-hourly mean value. In (a) the data correspond to daytime (05:30 to 20:30), when PPFD was higher than zero. GPP = gross primary production, R_{eco} = ecosystem respiration. (***) denotes a correlation significance level of $p < 0.001$.